Cell, Vol. 90, 959–966, September 5, 1997, Copyright ©1997 by Cell Press

The Directional Preference of Kinesin Motors Is Specified by an Element outside of the Motor Catalytic Domain

Ryan B. Case,† Daniel W. Pierce,*† Nora Hom-Booher,* Cynthia L. Hart,* and Ronald D. Vale*†‡
*Howard Hughes Medical Institute and the
†Departments of Pharmacology and Biochemistry
University of California
San Francisco, California 94143

Summary

Members of the kinesin superfamily share a similar motor catalytic domain yet move either toward the plus end (e.g., conventional kinesin) or the minus end (e.g., Ncd) of microtubules. The structural features that determine the polarity of movement have remained enigmatic. Here, we show that kinesin's catalytic domain (316 residues) in a dimeric construct (560 residues) can be replaced with the catalytic domain of Ncd and that the resultant motor moves in the kinesin direction. We also demonstrate that this chimera does not move processively over many tubulin subunits, which is similar to Ncd but differs from the highly processive motion of conventional kinesin. These findings reveal that the catalytic domain contributes to motor processivity but does not control the polarity of movement. We propose that a region adjacent to the catalytic domain serves as a mechanical transducer that determines directionality.

Introduction

The kinesin superfamily of ATP-hydrolyzing motor proteins are involved in membrane motility (Bloom and Endow, 1995; Hirokawa, 1996), chromosome segregation (Vernos and Karsenti, 1996; Walczak and Mitchison, 1996), microtubule dynamics (Walczak et al., 1996), ciliogenesis (Walther et al., 1994; Morris and Scholey, 1997), and intracellular signaling (Robbins et al., 1997; Sisson et al., 1997). All members of the superfamily share a similar ~320 amino acid domain (30%–40% aa identity) that contains the nucleotide and microtubule binding sites (termed here the "catalytic domain"), which can be positioned N-terminally, internally, or C-terminally in the polypeptide chain (Bloom and Endow, 1995). Adjacent to the catalytic domain is a 20–40 amino acid region termed the "neck," which is thought to work in concert with the catalytic domain to produce movement (Vale and Fletterick, 1997). The neck domains are highly conserved in subclasses of related kinesin motors but are not conserved throughout the superfamily (Vale and Fletterick, 1997). We refer to the region consisting of the catalytic domain and the neck as the functional "motor domain." Regions beyond the motor domain are involved in activities such as oligomerization and docking onto intracellular cargo.

A remarkable feature of the kinesin superfamily is that it contains members that move in opposite directions along microtubules (Bloom and Endow, 1995). Eleven kinesins with N-terminal motor domains (e.g., see Vale et al., 1985; Sawin et al., 1992; Cole et al., 1993) and one internal motor domain kinesin (KIF2) (Noda et al., 1995) have been shown to move to the plus end of microtubules. In contrast, four kinesins with C-terminal motor domains were demonstrated to be minus end–directed motors (e.g., see McDonald et al., 1990; Walker et al., 1990; Endow et al., 1994; Kuriyama et al., 1995). Unlike the kinesin superfamily, myosin and dynein motors have thus far been found to move in only one direction along actin filaments and microtubules, respectively.

What mechanism underlies the directional preference of kinesin motors? The simplest possibility is that plus end– and minus end–directed motor domains bind in reverse orientations on the microtubule. However, cryo-electron microscopy (cryo-EM) studies show that the orientations of Drosophila Ncd (a minus-end motor [McDonald et al., 1990; Walker et al., 1990]) and conventional kinesin (a plus-end motor [Vale et al., 1985]) are nearly identical (Arnal et al., 1996; Hirose et al., 1995, 1996). Other models have proposed that a difference in the timing of strong and weak binding states within the enzymatic cycle could give rise to opposite directions of movement (Taylor, 1993), but these have not received strong experimental support (Lockhart and Cross, 1994; Shimizu et al., 1995). A third class of models proposes that plus end– and minus end–directed motors develop different conformational change–driven "power strokes." Suggestive of this possibility, cryo-EM of microtubule-bound Ncd dimers and conventional kinesin dimers reveals that one of the two heads is detached and that the detached heads of Ncd and kinesin are positioned closer toward the minus end and plus end, respectively (Arnal et al., 1996; Hirose et al., 1996). This different posturing may help to bias the detached head to rebind to a tubulin subunit in opposite directions along the microtubule (Hackney, 1994; Arnal et al., 1996; Hirose et al., 1996).

To decipher the structural elements that determine directionality, Stewart et al. (1993) truncated Ncd and kinesin and positioned the motor domains at either the N or C termini of fusion proteins. They showed that the position of the motor domain in the polypeptide chain does not influence directionality and that the minimal motor domains of kinesin and Ncd (including the neck regions) are sufficient to dictate the polarity of movement. Recently, the crystal structures of the Ncd and conventional kinesin motor domains were determined (Kull et al., 1996; Sablin et al., 1996). The secondary structural elements of the catalytic domains closely superimpose, although some surface loops are different. The class-specific neck domains (which were not visible in the electron density maps of the published crystal structures) must also differ from one another, since the neck emerges C-terminal to the catalytic domain in conventional kinesin but N-terminal to this domain in the case of Ncd.

‡To whom correspondence should be addressed.

In this study, we have examined the structural determinants of directionality by generating chimeras of conventional kinesin and Ncd. We report that directionality is not governed by the motor catalytic domain, since a chimera composed of the entire Ncd catalytic domain flanked by adjacent kinesin sequences moves in the kinesin direction. In contrast, the source of the catalytic domain is important for processivity (long distance movement of a single motor molecule without detachment), since this phenomenon is exhibited by kinesin but not by Ncd or the chimera. These results also show that the catalytic domain is modular and can be coupled to neck regions of evolutionarily distant motors.

Results

Motility of Ncd-Kinesin Chimeras

Chimeric proteins of human conventional kinesin and Drosophila Ncd were generated based upon differences noted in the crystal structures of the two motors. Sablin et al. (1996) suggested that the class-specific neck regions adjacent to the motor catalytic domain might be involved in mechanical amplification and possibly directional bias. In the case of Ncd, the class-specific, conserved neck region consists of ~10–15 residues that precede the first β strand (β1) of the catalytic domain, whereas in kinesin, the conserved neck region follows the final helix (α6) (Figure 1) (Sablin et al., 1996). Although at opposite ends of the polypeptide, the N and C termini of the catalytic domain are located <10 Å apart in the three-dimensional structure. To test the idea that the necks are involved in directional preference, the catalytic domain of kinesin (β1 to α6; aa 8–322) was replaced with the corresponding region of Ncd (aa 348–667) (junctions indicated by arrows in Figure 1). The resultant chimera (NK-1) consists of the first seven amino acids of kinesin; the complete catalytic domain of Ncd; and the neck, flexible linker, and first coiled-coil stalk domains of kinesin (Bloom and Endow, 1995) (Figure 1). A second notable difference between Ncd and kinesin is an N-terminal, three-stranded β-sheet subdomain located near where the necks emerge from the catalytic domain. This subdomain contains two divergent loops (L1, L2) (Sablin et al., 1996) (Figure 1). To test whether the necks might act in concert with this class-specific subdomain, a chimera (NK-2) was prepared that consisted of N-terminal kinesin sequence to the end of the subdomain (aa 1–48), Ncd sequence from β2 to the end of α6 (aa 399–667), and then C-terminal kinesin sequence as described for NK-1 (Figure 1). A third major difference between the kinesin and Ncd crystal structures is in L11, which is a well-ordered surface loop stabilized by two antiparallel β strands in Ncd (Figure 1) but is disordered and appears to emerge at a different orientation in kinesin. This loop is considered to be part of the critical "switch II" region that changes conformation during the enzymatic cycle (Sablin et al., 1996; Vale, 1996) and hence could play a role in directionality. To test this possibility, Ncd L11 (aa 586–597) was substituted for kinesin L11 (aa 237–252) in the chimera NK-3 (Figure 1), which otherwise contains kinesin sequence.

All three chimeric constructs expressed soluble protein in E. coli, and proteins were purified by metal affinity and anion exchange chromatography. Motor activity of the chimeric proteins was tested by adsorbing them onto a glass coverslip and observing the movement of fluorescently labeled microtubules over the motor-coated surface. NK-1 and NK-3 generated microtubule gliding on the surface at rates of 50 ± 5 and 30 ± 3 nm/sec, respectively (Table 1). These rates are only ~3-fold slower than a Ncd fusion protein with green fluorescent protein (Ncd-GFP; 140 ± 10 nm/sec) but are more than an order of magnitude slower than wild-type kinesin (K560; 550 ± 140 nm/sec). With NK-2, microtubules were bound to the surface but did not move over a 45 min observation period, indicating that the N-terminal subdomain of kinesin is incompatible with the remainder of the Ncd catalytic domain. In contrast, the motility observed with NK-3 and NK-1 indicates that the switch II loop and catalytic domain of Ncd can function in the context of adjacent kinesin sequence.

To examine the direction of motor movement, motility assays were performed using polarity-marked microtubules that consist of a brightly labeled fluorescent segment at the minus end and a more dimly labeled segment at the plus end (Hyman, 1991). For wild-type kinesin (K560), the brightly labeled segment at the minus end was leading in the direction of movement, which indicates relative motion of the motors toward the plus end of the microtubule (Table 1). The polarity-marked microtubules moved in the opposite direction along surfaces coated with the Ncd-GFP fusion protein (Table 1). In the case of the two chimeras, NK-1 and NK-3, most or all microtubules moved across the surface with their minus ends leading (Figure 2; Table 1), indicating that both chimeras are plus end–directed motors like conventional kinesin. The plus end–directed motion induced by the NK-1 chimera is particulary remarkable, since the entire catalytic domain belongs to Ncd. This finding indicates that the catalytic domain does not specify the direction of movement.

Analysis of Motor Processivity

Conventional kinesin is a highly processive motor, and individual motor molecules can move unidirectionally along >100 tubulin subunits before detaching and diffusing away from the microtubule (Howard et al., 1989; Block et al., 1990; Hackney, 1995; Vale et al., 1996). Processivity is thought to involve a coordinated "hand-over-hand" mechanism of the two motor domains in the kinesin dimer (Hackney, 1994; Berliner et al., 1995; Vale et al., 1996). Processivity has not been examined for other members of the kinesin superfamily. Thus, we examined the processivity of single Ncd-GFP molecules and then determined whether the NK-1 chimera behaves more like kinesin or Ncd.

Movement of individual fluorescently labeled kinesin molecules along microtubules can be observed directly (Vale et al., 1996) using total internal reflection (TIR) microscopy (Funatsu et al., 1995). To observe single motor molecule dynamics in this study, we prepared motor-GFP fusions, since previous studies have shown that single GFP molecules (the S65T variant) can be detected by TIR microscopy (Pierce et al., 1997). For the wild-type kinesin and the NK-1 chimera, GFP was

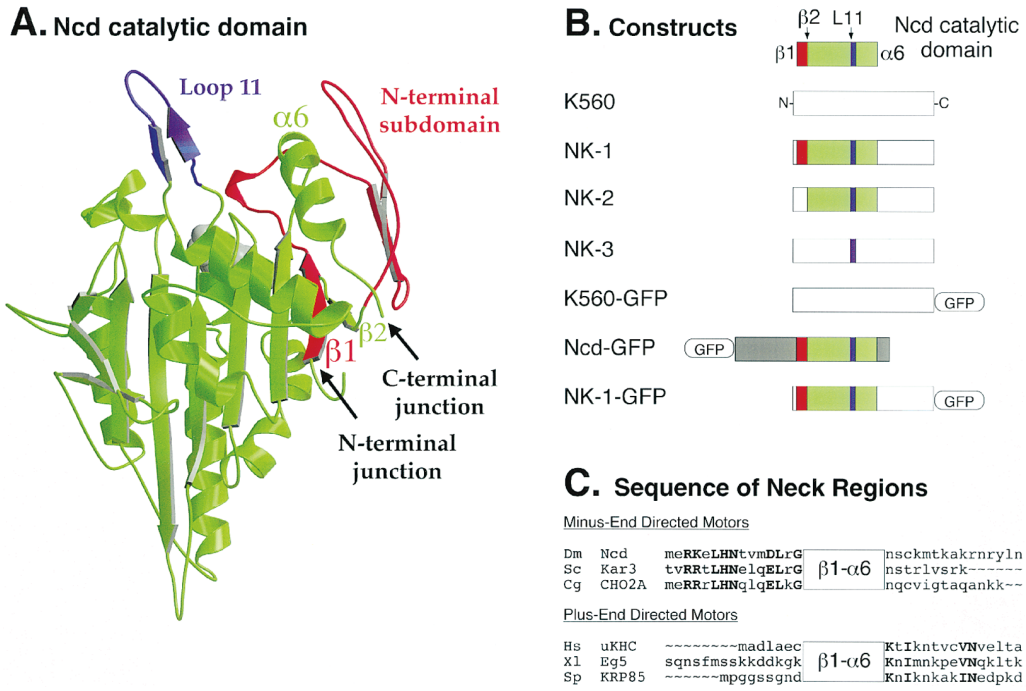

Figure 1. Chimeras between Drosophila Ncd (a Minus-End Motor) and Human Conventional Kinesin (a Plus-End Motor)

Kinesin 1–560 aa (K560) was used as a host construct for substituting regions of the Ncd catalytic domain. K560 contains the catalytic domain, the neck region, a flexible linker, the first coiled-coil domain of the kinesin stalk, followed by a 6×His tag for purification. In the chimera NK-1, the entire superfamily-conserved catalytic domain (β1–α6; aa 348–667) was substituted for the equivalent domain of kinesin (β1–α6; aa 8–322). The N- and C-terminal junctions in the Ncd structure (residues 348 and 667) are indicated by the arrows in (A). In NK-2, the catalytic motor domain of Ncd from β2 to α6 (aa 399–667) was substituted for the corresponding region of kinesin (aa 49–322). The N-terminal region from β1 to β2 (red in [A]) consists primarily of a subdomain that differs in structure between kinesin and Ncd (Sablin et al., 1996). In NK-3, loop 11 of Ncd (aa 586–597 [blue]; the most dissimilar loop in the kinesin and Ncd crystal structures) was substituted for the corresponding region of kinesin (aa 237–252). (B) shows all of the constructs used in this study. Kinesin sequence is indicated in the open boxed regions. Ncd sequence is shown in color (the catalytic domain) and by shading (the nonmotor domain). Color coding for the catalytic domain elements corresponds to those shown in (A). In (C), the amino acid sequences N-terminal to β1 and C-terminal to α6 of the superfamily-conserved catalytic domain are indicated for three minus end–directed motors (DmNcd: McDonald et al., 1990; Walker et al., 1990; CgCHO2: Kuriyama et al., 1995; ScKAR3: Endow et al., 1994) and three plus end–directed motors (SpKRP85: Cole et al., 1993; XlEg5: Sawin et al., 1992; HsuKHC: Vale et al., 1985). These alignments indicate that the minus end–directed motors contain class-specific neck residues N-terminal to the catalytic domain while plus end–directed motors contain conserved neck residues C-terminal to the catalytic domain. The conserved glycine (G) before β1 is residue 347, 385, and 259 in DmNcd, ScKar3, and CgCHO2A, respectively. The conserved lysine (K) following the α6 is residue 323, 407, and 340 in HsuKHC, XlEg5, and SpKRP85, respectively. Residues in bold capital letters indicate class-specific, conserved residues.

fused C-terminally to residue 560. In the case of Ncd, GFP was fused N-terminally to residue 236, which retains ~3/4 of the Ncd coiled-coil stalk and the complete motor domain but lacks the N-terminal domain that bundles microtubules (Chandra et al., 1993). This GFP fusion method is advantageous compared to fluorescent dye modification, which tends to inactivate the Ncd catalytic domain. Hydrodynamic and single fluorescent spot intensity analysis (see Experimental Procedures) indicated that K560-GFP and Ncd-GFP are dimers under conditions of the assay. K560-GFP, Ncd-GFP, and NK-1-GFP all produced movement in gliding assays where multiple motors interact simultaneously with a microtubule (Table 1). Thus, all GFP fusion proteins were active motors.

When K560-GFP was combined with axonemal microtubules and ATP, individual fluorescent spots could be easily observed binding to and moving unidirectionally along the axoneme, as shown previously (Pierce et al., 1997). At a concentration of 1.3 nM K560-GFP, detectable movements (>300 nm) occured at a frequency of 3.0 min^{-1} μm^{-1} axoneme length (n = 360 events) with a velocity of 410 ± 150 nm/sec (mean ± SD; n = 63). The travel distance was exponentially distributed with a mean of 1070 nm. At 10 nM motor, moving spots decorated the axonemes and fluoresence accumulated at the microtubule plus end (Figure 3A). In contrast, processive movement was never observed for Ncd-GFP and NK-1-GFP at motor concentrations ranging from 1 to 50 nM and with a variety of buffer conditions (see Experimental Procedures). At 10 nM NK-1-GFP and Ncd-GFP, fluorescent spots did not associate with axonemes at more than background levels, indicating that microtubule associations must be very transient. No accumulation of fluorescence was observed at either axoneme end (Figure 3A). The failure to observe processive motion was not likely due to a masking effect from a large population of inactive motors in the preparation, since motility of a trace amount of K560-GFP (2% mole fraction) could be easily observed when added to 20 nM Ncd-GFP or NK-1-GFP. The capacity of Ncd-GFP and NK-1-GFP to bind to microtubules in this assay was

Table 1. Motility of Kinesin, Ncd, and Kinesin-Ncd Chimeras

Construct	MT Gliding (nm/sec)	Directionality		Single-Molecule Run Length (nm)
		Plus	Minus	
Kinesin K560	550 ± 140	96	0	
NK-1	50 ± 5	92	0	
NK-2	0	—	—	
NK-3	30 ± 3	67	1	
K560-GFP	370 ± 50	Not tested		1070 ± 260
NCD-GFP	140 ± 10	0	91	<50
NK-1-GFP	60 ± 10	Not tested		<50

Motility assays are described in the Experimental Procedures. Microtubule gliding velocities (mean and standard deviations) were measured for 25–50 microtubules. Direction of movement was determined using polarity-marked microtubules; the single minus-end movement measured for NK-3 was probably due to either aberrant polymerization of artifactual annealling between a dim and a bright microtubule. For determining the run length of molecules in the single-molecule fluorescence motility assay, travel lengths of single K560-GFP molecules (n = 63) were measured and an exponential curve was fit to the distribution as described in Vale et al. (1996). The decay constant of the exponential provides the mean run length, and the error of the fit is indicated. The velocity of moving kinesin-GFP spots was 410 ± 150 nm/sec. Although processive movement was not measured for Ncd-GFP and NK-1-GFP, an upper bound of 50 nm mean run length can be estimated since an observable fraction of runs would exceed the 250 nm threshold for detection of movement. This upper bound can be further reduced to ~20 nm for NK-1-GFP based upon the association times as described in the text.

demonstrated by inducing a strong microtubule binding state by depleting ATP, which resulted in the association of the majority of fluorescent molecules with the axoneme (Figure 3B).

Single K560-GFP molecules move at a velocity similar to that observed in the microtubule gliding assay (Table 1). If single Ncd-GFP and NK-1-GFP molecules also move at their corresponding microtubule gliding velocity of ~140 and 60 nm/sec, they should remain bound to the axoneme for ~0.33 sec (10 video frames) while executing run lengths of ~50 and ~20 nm, respectively. Since associations of this duration can be easily detected but were rarely observed, the run lengths are unlikely to be >6 tubulin subunits (each α/β tubulin subunit is ~8 nm). In further support of this conclusion, if Ncd-GFP and NK-1-GFP had mean run lengths of ~50 nm with an exponential distribution, then a detectable number of spots should have been observed moving >250 nm (our spatial detection limit) in 10 min of observation. These results indicate that Ncd, unlike conventional kinesin, is not a highly processive motor. Therefore, with regard to single molecule motility, NK-1 is more akin to Ncd than to kinesin, implying that the catalytic domain influences motor processivity.

Discussion

In this study, we have explored the structural determinants for motor directionality and processivity by preparing chimeras of conventional kinesin and Ncd. Our results show that a chimera containing the entire motor catalytic domain of Ncd flanked by adjacent kinesin sequences will move toward the microtubule plus end.

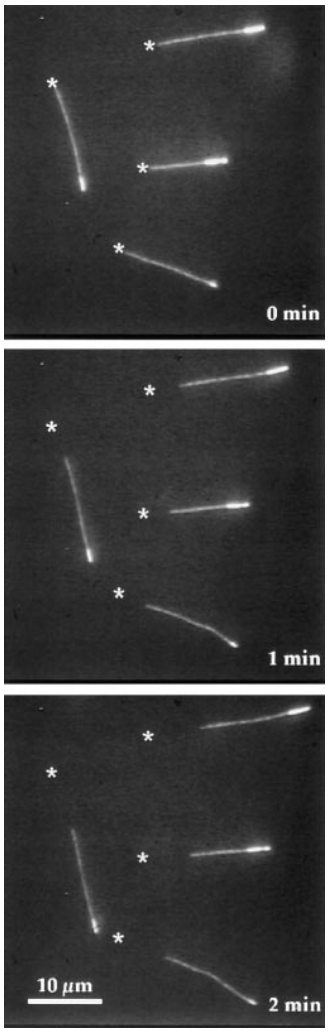

Figure 2. The NK-1 Chimera Is a Plus End–Directed Microtubule Motor

Polarity-marked microtubules are shown with a bright fluorescent segment at the minus end and a dimmer fluorescent segment at the plus end. These microtubules move over NK-1-coated surfaces with the minus end leading, indicating the relative movement of the motors toward the plus end of the microtubule. Asterisks (*) indicate the initial starting position of these microtubules.

This result strongly suggests that elements outside of the catalytic domain determine the directional preference of the motor. In contrast, this chimera, like Ncd, fails to exhibit the high degree of processivity displayed by kinesin. This latter finding indicates that the motor catalytic domain likely contributes to the head-head coordination of the chemomechanical cycles that is thought to be required for processive motion (Hackney, 1994; Berliner et al., 1995; Vale et al., 1996). The difference in processivity of kinesin and Ncd may reflect their different biological roles in organelle transport and mitotic/meiotic spindle formation, respectively, since the efficiency of the latter process may not require that single motors move for long distances along microtubules.

Which elements of the kinesin sequence in the NK-1 chimera determine directionality? The seven kinesin

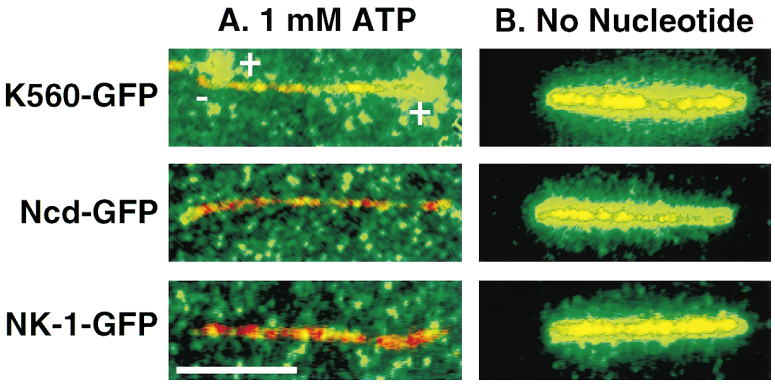

Figure 3. Single Molecule Fluorescence Motility Assays for K560-GFP, Ncd-GFP, and NK-1-GFP

Processive movement was evaluated by observing the interactions of single K560-GFP, Ncd-GFP, and NK-1-GFP molecules with axonemal microtubules using total internal reflection microscopy as described in the Experimental Procedures. Axonemes labeled with Cy5 dye are pseudocolored in red, and motor molecules fused to GFP are pseudocolored in green; areas of overlap appear yellow. For K560-GFP (10 nM) in 12 mM KPIPES (pH 6.8) buffer in the presence of ATP (1 mM), an accumulation of fluoresence is observed toward the microtubule plus ends ([A]; [+] symbols mark the plus ends of two axonemes in this field). After photobleaching to reduce the fluorescence intensity, this accumulation was found to be the result of numerous fluorescent spots binding to and moving along the microtubules unidirectionally (see Vale et al. [1996]). From the direction of movement of K560-GFP, the axoneme plus end can be assigned. In contrast, neither axonemal decoration, microtubule-end accumulation, nor movement of spots was observed for Ncd-GFP and NK-1-GFP at the same motor concentrations, suggesting transient associations (A). In the presence of apyrase (1 U/ml), which depletes nucleotide and promotes a strong microtubule binding state, K560-GFP, Ncd-GFP, and NK-1-GFP all strongly decorated the axonemal microtubules and very few free fluorescent spots were observed (B). All six images shown were obtained and processed identically, so brightness and contrast may be directly compared. Bar, 5 μm.

amino acids N-terminal to β1 of the catalytic domain are unlikely to do so, since they show neither length nor sequence conservation (Figure 1). In contrast, the neck region located C-terminally to the catalytic domain is highly conserved (see Figure 1) and has been proposed to serve as a mechanical transducer (Kull et al., 1996). The neck regions of kinesin and Ncd are not visible in the current crystal structures. However, the secondary structure of synthetic peptides corresponding to the conserved 40 aa neck region of kinesin have been analyzed (Morii et al., 1997; Tripet et al., 1997). The first 10 residues, which are conserved in all known plus end–directed motors, have a high propensity to form a β-sheet structure, while the subsequent 30 residues form an α-helical coiled-coil that can dimerize two kinesin motor domains (Huang et al., 1994). The importance of the neck in kinesin motility is demonstrated by the finding that successive C-terminal deletions of this region result in a decrease in motor velocity and a loss of processivity (Vale et al., 1996). Furthermore, double and triple alanine mutations within the first 10 neck residues of kinesin virtually abolish motor-induced microtubule gliding. A mutant NK-1 protein containing a deletion of kinesin neck residues 323–332 also failed to display motility, indicating that this region is important in the chimera as well (R. B. C., B. Ly, and R. D. V., unpublished data).

A previous study by Stewart et al. (1993) examined directionality of truncated kinesin and Ncd motors and concluded that directionality is intrinsic to the conserved motor domain rather than being a property of adjacent sequences or domain organization. While their conclusion would seem inconsistent with ours, the difference lies solely in how the motor domain is defined in the two studies. In the Stewart et al. work, the minimal Drosophila kinesin construct that conferred plus-end directional motion contained residues 1–339, while the minimal Ncd construct that elicited minus-end directional motion contained residues 320–685 (both were GST fusion proteins). These regions were termed the "conserved motor region," but this definition preceded the extensive kinesin superfamily alignments and crystal structure information that are now available. In fact, these constructs consist of the superfamily-conserved catalytic domain as well as 9 and 13 residues of the class-specific neck regions of kinesin (corresponding to human kinesin residues 323–331) and Ncd (residues 335–347), respectively (see Figure 1C). Thus, the experiments of Stewart et al. are in no way inconsistent with ours. On the contrary, their results on the opposite directions of movement of minimal Ncd and kinesin constructs, taken together with our findings, further strengthen the conclusion that the neck regions adjacent to the catalytic domain specify the direction of motion.

This study suggests a model in which the motor catalytic domain functions as an allosteric core that conveys information from the nucleotide pocket to a nearby mechanical transducer. Unexpectedly, this conformational change pathway must be sufficiently modular such that the catalytic domain of one motor class (Ncd) can communicate with the mechanical transducer of an evolutionarily distant motor class (conventional kinesin). The finding that the NK-3 chimera has motor activity is also remarkable and indicates that the switch II loop (L11), which is structurally distinct in kinesin and Ncd, is modular and partially functional in the context of different catalytic domains. The conformational changes that take place during the kinesin enzymatic cycle remain to be elucidated. However, the N and C termini of the catalytic core are close in space (Figure 1), and thus the different necks of Ncd and kinesin conceivably could communicate with the same elements of the catalytic domain that change conformation during the ATPase cycle.

While this study argues that sequences outside of the motor domain specify directional preference, the exact mechanism of the directional bias remains to be elucidated. Cryo-EM studies have been interpreted to suggest that the neck regions of kinesin and Ncd are oriented differently (Arnal et al., 1996; Hirose et al., 1996). Hirose et al. (1995) have also suggested that the neck

region may change conformation in different nucleotide states. Such studies support the speculation that the neck may be important for biasing motor movement along the microtubule. Atomic resolution structures of the neck regions of minus end– and plus end–directed motors in different nucleotide states as well as further mapping studies of the "directionality element" will be important next steps for understanding the detailed mechanism of directional motion.

Experimental Procedures

Expression Constructs

A human conventional kinesin construct comprising residues 1–560 with a C-terminal 6 histidine (6×His) tag was cloned into pET17B (Novagen, Inc.). The chimera NK-1 was constructed by performing PCR on the GST-MC1 construct (Chandra et al., 1993) with the 5′ oligo corresponding to aa 348–359 and the 3′ oligo corresponding to aa 656–667 to generate PCR product 1 (encoding aa 348–667). A second PCR reaction was performed on the K560-6×His vector above using a 5′ oligo corresponding to aa 323–333 and a 3′ oligo corresponding to aa 7 and extending 14 bp into the vector promoter to generate a 3.9 kb product (PCR product 2) that included N- and C-terminal kinesin sequences as well as the intervening vector sequence. Products 1 and 2 were treated with alkaline phosphatase and the Klenow polymerase fragment to ensure blunt ends. The two PCR products were then ligated and transformed in DH5α cells. The C-terminal junction of the ligated product had a base-pair deletion that was later repaired by PCR mutagenesis. The repaired chimera was then subcloned between Nde1 (aa 1) and Mun1 (aa 407) sites into the K560-6×His pET17B vector to eliminate any PCR-induced errors in the vector. NK-2 was generated by the same strategy as indicated above with the exception that the 5′ oligo for PCR product 1 corresponded to aa 49–60 and the 3′ oligonucleotide for PCR product 2 corresponded to aa 48–37. The NK-3 construct was generated by Stratagene QuikChange protocol (Stratagene, Inc.) using oligonucleotides that substituted the Ncd L11 sequence (aa 586–597) for the kinesin L11 sequence (aa 237–252) in the K560-6×His pET17B vector. The remainder of the cloning was as described in Woehlke et al. (1997). All coding regions were confirmed by DNA sequencing.

For GFP fusion proteins, PCR was used to introduce: (1) a 5′ Nde1 site and a 3′ Kpn1 site at aa 560 of human ubiquitous kinesin and NK-1, and (2) a 5′ Kpn1 site and a 3′ 6×His tag plus an Xho1 site to GFP mutant S65T (from R. Tsien [UCSD]). K560 and NK-1 were then fused to GFP at the introduced Kpn1 site (which adds a Gly-Thr linker sequence) and cloned into pET17b between the Nde1 and Xho1 sites. To make the Ncd-GFP fusion, a 5′ Kpn1 site and a 3′ Xho1 site were added to Ncd aa 236–700, and a 5′ Nhe1 site plus 6×His tag and 3′ Kpn1 site were added to GFP (again adding a Gly-Thr linker sequence) via PCR. These products were joined together into the Nhe1–Xho1 sites of pET17b. All PCR-derived sequences were confirmed by DNA sequencing.

Bacterial Protein Expression

K560 and Chimeras

Constructs were transformed into E. coli strain BL21(DE3), grown in TPM-ampicillin (20 g/l tryptone, 15 g/l yeast extract, 8 g/l NaCl, 10 mM glucose, 2 g/l Na_2HPO_4, 1 g/l KH_2PO_4, and 100 μg/ml ampicillin) at 24°C to OD_{600} of 1, and then protein expression was induced for 9 hr with 0.1 mM IPTG. Cells were lysed by French press (0.8 MPa) in 50 mM $NaPO_4$ (pH 8), 20 mM imidazole, 250 mM NaCl, 1 mM $MgCl_2$, 0.5 mM ATP, 10 mM β-mercaptoethanol (βME), leupeptin (1 μg/ml), pepstatin (1 μg/ml), chymostatin (1 μg/ml), aprotinin (1 μg/ml), and 0.25 mg/ml Pefabloc (Boehringer Mannheim) (50 ml of buffer per 2 l of culture). The supernatant from a 28,000 × g, 30 min centrifugation was collected and incubated with Ni-NTA resin (Qiagen, Inc.) for 1 hr at 4°C (1–2.5 ml of resin per 50 ml of supernatant). The mixture was then transferred to a disposable column, and the resin was washed with 50 ml of 50 mM $NaPO_4$ (pH 6), 250 mM NaCl, 1 mM $MgCl_2$, 0.1 mM ATP, and 10 mM βME. Proteins were eluted with 50 mM $NaPO_4$, 500 mM imidazole-Cl, 250 NaCl, 1 mM $MgCl_2$, 0.1 mM ATP, and 10 mM βME (pH 7.2). The peak fractions were then diluted 5-fold into column buffer supplemented with 50 mM NaCl and further purified by Mono-Q chromatography using a 20 ml 0.1–1.0 M gradient in 25 mM NaPIPES (pH 6.8; for K560) or 10 mM $NaPO_4$ (pH 7.2; for the chimeras) with 2 mM $MgCl_2$, 1 mM EGTA, 1 mM DTT, and 25 μM ATP. K560 and the chimeras eluted at 0.35 M NaCl.

GFP Fusion Proteins

Cells were grown at 37°C to OD_{600} of 1–2 and cooled to 23°C, and then protein expression was induced for 9–14 hr with 0.2 mM IPTG. Cell lysis conditions and Ni-NTA chromatography were as described above. The K560-GFP and NK-1-GFP fusion proteins were purified by Mono-Q chromatography with elution at 0.35 M NaCl in a 16 ml 0.2–1.0 M gradient in 25 mM NaPIPES (pH 6.8; K560-GFP) or 10 mM $NaPO_4$ (pH 7.2; NK-1-GFP) with 2 mM $MgCl_2$, 1 mM EGTA, 1 mM DTT, and 0.1 mM ATP. Ncd-GFP was further purified by Mono-S chromatography with elution at 0.3 M NaCl in a 30 ml 0.1–1.1 M NaCl gradient in 10 mM $NaPO_4$ (pH 7.2), 2 mM $MgCl_2$, 1 mM EGTA, 1 mM DTT, and 0.1 mM ATP. The motor-GFP fusion proteins were then subjected to an additional microtubule affinity purification step by incubating with microtubules and 1 mM AMPPNP, centrifuging the motor-microtubule complex and releasing the active motor from the microtubule with 5 mM MgATP/200 mM KCl.

For all preparations, 10%–20% sucrose was added to peak fractions before freezing and storage in liquid nitrogen. Protein concentrations were calculated by running the kinesin along with a BSA standard curve on a SDS–polyacrylamide gel, staining with Coomassie, capturing the gel image with a CCD camera, and then measuring optical densities using the computer program NIH Image.

Motility Assays

Microtubule gliding assays for K560 were performed as previously described (Woehlke et al., 1997). For the chimeras and K560 generated in this study, motors from the peak Mono-Q fractions were adsorbed onto glass surfaces of microscope flow cells at concentrations of 0.5–10 μM. For motor-GFP fusion proteins, affinity-purified anti-GFP polyclonal antibodies (0.5 mg/ml) were first adsorbed onto the glass surface, the flow cell was washed with buffer, and the motors were then allowed to bind to the antibody-coated surface. Motility buffer was introduced containing 15 mM NaMOPS (pH 7), 50 mM NaCl, 20 μM taxol, ~10 μg/ml rhodamine-labeled microtubules (Hyman et al., 1990), 1 mM ATP, 1 mM EGTA, 2 mM $MgCl_2$, 1 mM DTT, 2 mg/ml casein, and an oxygen depletion system composed of 22 mM glucose, 0.5% β-mercaptoethanol, 0.2 mg/ml glucose oxidase, and 36 μg/ml catalase (Harada et al., 1990). Similar gliding motility was also observed in the lower ionic strength buffers employed in the single molecule fluorescence motility assays.

Polarity-marked microtubules (Hyman, 1991) were prepared by first polymerizing short microtubules from rhodamine-tubulin and 0.5 mM GMPCPP (a nonhydrolyzable GTP analog). These brightly labeled microtubules were then used as seeds to polymerize a more dimly labeled microtubule segment with 0.1 mg/ml rhodamine-labeled tubulin, 1.5 mg/ml unlabeled tubulin, and 1.5 mg/ml NEM-modified tubulin (Hyman et al., 1990), which inhibits minus-end growth. Polarity-marked microtubules were used in the same assays described above.

For the single-molecule fluorescence motility assay, motor-GFP proteins were diluted to a concentration of 1–50 nM in a buffer containing 1 mM ATP, 1 mM EGTA, 2 mM $MgCl_2$, 7.5 mg/ml bovine serum albumin (BSA) as carrier protein, and the oxygen depletion system described above. Kinesin-GFP was standardly assayed in the above solution with 12 mM KPIPES (pH 6.8). Movement of Ncd-GFP and NK-1-GFP was not detected in a variety of buffer conditions including 12 mM KPIPES (pH 6.8), 12 mM KMOPS (pH 7), 50 mM KMOPS (pH 7), and 50 mM KMOPS (pH 7) with 50 mM NaCl.

For Ncd-GFP, sucrose density gradient centrifugation (5.84 Svedberg) and gel filtration chromatography (3.48×10^{-7} cm^2/sec) were performed (Huang et al., 1994), revealing a molecular weight of 151 kDa that is close to that predicted for a dimer (161 kDa). Moreover, prior analysis of single-spot fluorescence intensities by TIR microscopy show a 2.1- and 1.9-fold greater signal for Ncd-GFP and K560-GFP compared to a monomeric construct (unc104-GFP) (Pierce et al., 1997). This indicates that K560 kinesin and Ncd

are dimers under the conditions of the single-molecule motility assay.

Microscopy and Analysis

For microtubule gliding assays, rhodamine-labeled microtubules were illuminated with a 100 W mercury lamp and imaged by epifluorescence microscopy using a 60×, 1.4 NA objective (Olympus, Inc). The image was projected onto a silicon-intensified target camera (Hamamatsu, Inc.) and then recorded onto sVHS tape. Velocities were measured using a custom computer program in which the ends of microtubules were manually marked with a mouse.

For single-molecule fluorescence imaging, 4 μl of assay mix described above was spotted onto a cleaned quartz slide, covered with an 18 mm coverslip, sealed with rubber cement, and imaged on a low background TIR optical bench microscope constructed by the authors (Pierce and Vale, 1997). Briefly, an argon-ion laser was used at 488 nm and 5 mW to excite GFP, and a HeNe laser was operated at 0.4 mW to excite sea urchin axonemes (prepared as described by Gibbons and Fronk [1979]) and labeled with Cy5 dye (Vale et al., 1996). Laser illumination was passed through a λ/4 plate set to produce circularly polarized light and focused by a 25 cm lens at an appropriate angle through a prism to produce total internal reflection and evanescent field illumination of an ~30 × 40 mm area at the sample (Funatsu et al., 1995). Fluorescence was collected by a Nikon PlanApo 100/1.4 objective, collimated, passed through custom-designed dichroic mirror and barrier filters, and focused onto a CCD camera coupled to a selected SR UB Gen3+ intensifier tube from Stanford Photonics Inc. Data was recorded to video tape after contrast enhancement by an Argus-20 image processor (Hamamatsu Photonics, Inc.). Travel distances of moving spots of kinesin-GFP were measured as described previously (Vale et al., 1996). Behavior of single GFP molecule fluorescence is described elsewhere (Pierce et al., 1997).

Acknowledgments

We thank Arshad Desai for advice on preparing polarity-marked microtubules and video capture. We are grateful to C. Coppin, K. Dell, D. Friedman, B. Govindan, L. Romberg, and C. Walczak for providing comments on the manuscript. R. C. is supported by a National Institutes of Health training grant, and D. W. P. receives support from a Jane Coffin Childs Fellowship.

Received July 24, 1997; revised August 11, 1997.

References

Arnal, I., Metoz, F., DeBonis, S., and Wade, R.H. (1996). Three-dimensional structure of functional motor proteins on microtubules. Curr. Biol. *6*, 1265–1270.

Berliner, E., Young, E.C., Anderson, K., Mahtani, H., and Gelles, J. (1995). Failure of a single-headed kinesin to track parallel to microtubule protofilaments. Nature *373*, 718–721.

Block, S.M., Goldstein, L.S., and Schnapp, B.J. (1990). Bead movement by single kinesin molecules with optical tweezers. Nature *348*, 348–352.

Bloom, G., and Endow, S. (1995). Motor Proteins 1: kinesin. Prot. Profile *2*, 1112–1138.

Chandra, R., Salmon, E.D., Erickson, H.P., Lockhart, A., and Endow, S.A. (1993). Structural and functional domains of the Drosophila ncd microtubule motor protein. J. Biol. Chem. *268*, 9005–9013.

Cole, D.G., Chinn, S.W., Wedaman, K.P., Hall, K., Vuong, T., and Scholey, J.M. (1993). Novel heterotrimeric kinesin-related protein purified from sea urchin eggs. Nature *366*, 268–270.

Endow, S.A., Kang, S.J., Satterwhite, L.L., Rose, M.D., Skeen, V.P., and Salmon, E.D. (1994). Yeast Kar3 is a minus-end microtubule motor protein that destabilizes microtubules preferentially at the minus ends. EMBO J. *13*, 2708–2713.

Funatsu, T., Harada, Y., Tokunaga, M., Saito, K., and Yanagida, Y. (1995). Imaging of single fluorescent molecules and individual ATP turnovers by single myosin molecules in aqueous solution. Nature *374*, 555–559.

Gibbons, I.R., and Fronk, E. (1979). A latent adenosine triphosphatase form of dynein 1 from sea urchin sperm flagella. J. Biol. Chem. *254*, 187–196.

Hackney, D.D. (1994). Evidence for alternating head catalysis by kinesin during microtubule-stimulated ATP hydrolysis. Proc. Natl. Acad. Sci. USA *91*, 6865–6869.

Hackney, D.D. (1995). Highly processive microtubule-stimulated ATP hydrolysis by dimeric kinesin head domains. Nature *377*, 448–450.

Harada, Y., Sakurada, K., Aoki, T., Thomas, D.D., and Yanagida, T. (1990). Mechanochemical coupling in actomyosin energy transduction studied by in vitro movement assay. J. Mol. Biol. *216*, 49–68.

Hirokawa, N. (1996). Organelle transport along microtubules—the role of KIFs. Trends Cell Biol. *6*, 135–141.

Hirose, K., Lockhart, A., Cross, R.A., and Amos, L.A. (1995). Nucleotide-dependent angular change in kinesin motor domain bound to tubulin. Nature *376*, 277–279.

Hirose, K., Lockhart, A., Cross, R.A., and Amos, L.A. (1996). Three-dimensional cryoelectron microscopy of dimeric kinesin and ncd motor domains on microtubules. Proc. Natl. Acad. Sci. USA *93*, 9539–9544.

Howard, J., Hudspeth, A.J., and Vale, R.D. (1989). Movement of microtubules by single kinesin molecules. Nature *342*, 154–158.

Huang, T.G., Suhan, J., and Hackney, D.D. (1994). Drosophila kinesin motor domain extending to amino acid position 392 is dimeric when expressed in Escherichia coli. J. Biol. Chem. *269*, 16502–16507.

Hyman, A.A. (1991). Preparation of marked microtubules for the assay of the polarity of microtubule-based motors by fluorescence. J. Cell Sci. (Suppl.) *14*, 125–127.

Hyman, A., Dreschel, D., Kellogg, D., Salser, S., Sawin, K., Steffen, P., Wordeman, L., and Mitchison, T. (1990). Preparation of modified tubulins. Meth. Enzymol. *196*, 303–319.

Kull, F.J., Sablin, E.P., Lau, R., Fletterick, R.J., and Vale, R.D. (1996). Crystal structure of the kinesin motor domain reveals a structural similarity to myosin. Nature *380*, 550–555.

Kuriyama, R., Kofron, M., Essner, R., Kato, T., Dragas-Granoic, S., Omoto, C.K., and Khodjakov, A. (1995). Characterization of a minus end-directed kinesin-like motor protein from cultured mammalian cells. J. Cell Biol. *129*, 1049–1059.

Lockhart, A., and Cross, R.A. (1994). Origins of reversed directionality in the ncd molecular motor. EMBO J. *13*, 751–757.

McDonald, H.B., Stewart, R.J., and Goldstein, L.S. (1990). The kinesin-like ncd protein of Drosophila is a minus end–directed microtubule motor. Cell *63*, 1159–1165.

Morii, H., Takenawa, T., Arisaka, F., and Shimizu, T. (1997). Identification of kinesin neck region as a stable α-helical coiled-coil and its thermodynamic characterization. Biochemistry *36*, 1933–1942.

Morris, R.L., and Scholey, J.M. (1997). Heterotrimeric kinesin-II is required for the assembly of motile 9+2 ciliary axonemes in sea urchin embryos. J. Cell Biol., in press.

Noda, Y., Sato-Yoshitake, R., Kondo, S., Nangaku, M., and Hirokawa, N. (1995). KIF2 is a new microtubule-based anterograde motor that transports membraneous organelles distinct from those carried by kinesin heavy chain or KIF3A/B. J. Cell Biol. *129*, 157–167.

Pierce, D.W., and Vale, R.D. (1997). Assaying processive movement of kinesin by fluorescence microscopy. Meth. Enzymol., in press.

Pierce, D.W., Hom-Booher, N., and Vale, R.D. (1997). Imaging of individual green fluorescent proteins. Nature *388*, 338.

Robbins, D.J., Nybakken, K.E., Kobayashi, R., Sisson, J.C., Bishop, J.M., and Therond, P.P. (1997). Hedgehog elicits signal transduction by means of a large complex containing the kinesin-related protein Costal2. Cell *90*, 225–234.

Sablin, E.P., Kull, F.J., Cooke, R., Vale, R.D., and Fletterick, R.J. (1996). Crystal structure of the motor domain of the kinesin-related motor ncd. Nature *380*, 555–559.

Sawin, K.E., LeGuellec, K., Philippe, M., and Mitchison, T.J. (1992). Mitotic spindle organization by a plus-end-directed microtubule motor. Nature *359*, 540–543.

Shimizu, T., Sablin, E., Vale, R.D., Fletterick, R., Pechatnikova, E., and Taylor, E.W. (1995). Expression, purification, ATPase properties, and microtubule-binding properties of the ncd motor domain. Biochemistry *34*, 13259–13266.

Sisson, J.C., Ho, K.S., Suyama, K., and Scott, M.P. (1997). Costal2, a novel kinesin-related protein in the Hedgehog signaling pathway. Cell *90*, 235–245.

Stewart, R.J., Thaler, J.P., and Goldstein, L.S. (1993). Direction of microtubule movement is an intrinsic property of the motor domains of kinesin heavy chain and Drosophila ncd protein. Proc. Natl. Acad. Sci. USA *90*, 5209–5213.

Taylor, E.W. (1993). Variations on the theme of movement. Nature *361*, 115–116.

Tripet, B., Vale, R.D., and Hodges, R.S. (1997). Demonstration of coiled-coil interactions within the kinesin neck region using synthetic peptides: implications for motor activity. J. Biol. Chem. *272*, 8946–8956.

Vale, R.D. (1996). Switches, latches, and amplifiers: common themes of molecular motors and G proteins. J. Cell Biol. *135*, 291–302.

Vale, R.D., and Fletterick, R.J. (1997). The design plan of kinesin motors. Annu. Rev. Cell Dev. Biol. *13*, 745–777.

Vale, R.D., Schnapp, B.J., Mitchison, T., Steuer, E., Reese, T.S., and Sheetz, M.P. (1985). Different axoplasmic proteins generate movement in opposite directions along microtubules in vitro. Cell *43*, 623–632.

Vale, R.D., Funatsu, T., Pierce, D.W., Romberg, L., Harada, Y., and Yanagida, T. (1996). Direct observation of single kinesin molecules moving along microtubules. Nature *380*, 451–453.

Vernos, I., and Karsenti, E. (1996). Motors involved in spindle assembly and chromosome segregation. Curr. Opin. Cell Biol. *8*, 4–9.

Walczak, C.E., and Mitchison, T.J. (1996). Kinesin-related proteins at mitotic spindle poles: function and regulation. Cell *85*, 943–946.

Walczak, C.E., Mitchison, T.J., and Desai, A. (1996). XKCM1: a Xenopus kinesin-related protein that regulates microtubule dynamics during mitotic spindle assembly. Cell *84*, 37–47.

Walker, R.A., Salmon, E.D., and Endow, S.A. (1990). The *Drosophila* claret segregation protein is a minus-end directed motor molecule. Nature *347*, 780–782.

Walther, Z., Vashishtha, M., and Hall, J.L. (1994). The Chlamydomonas FLA10 gene encodes a novel kinesin-homologous protein. J. Cell Biol. *126*, 175–188.

Woehlke, G., Ruby, A.K., Hart, C.L., Ly, B., Hom-Booher, N., and Vale, R.D. (1997). Microtubule interaction site of the kinesin motor. Cell *90*, 207–216.